2010 International Pittsburgh Coal Conference
Istanbul, Turkey
October 11 – 14, 2010

NUMERICAL SIMULATION OF GASIFICATION PROCESS IN A CROSS-TYPE TWO-STAGE GASIFIER

Yau-Pin Chyou, Chang-Bin Huang, Yan-Tsan Luan
Nuclear Fuels and Materials Division
Institute of Nuclear Energy Research
Atomic Energy Council
Longtan, Taoyuan, Taiwan (R.O.C.)

Ting Wang
Energy Conversion & Conservation Center
University of New Orleans
New Orleans, Louisiana, USA

ABSTRACT

Numerical simulation of the oxygen-blown coal gasification process inside a cross-type two-stage (E-Gas like) gasifier is studied with the commercial CFD solver ANSYS FLUENT. The purpose of this study is to use CFD simulation to improve understanding of the gasification processes in the E-Gas like gasifier. In this paper, chemical reaction time is assumed to be faster than the time scale of the turbulence eddies. All the species are assumed to mix in the intermolecular level. The 3-D Navier-Stokes equations and species transport equations are solved with the eddy-breakup reaction model (instantaneous gasification). The influences of coal slurry concentration and O_2/coal ratio on the gasification process are investigated. Under the condition of feeding carbon being almost completely converted, low slurry concentration is preferred over high concentration if more H_2 is wanted with lower syngas temperature; while higher slurry concentration is preferable for producing more CO with higher syngas temperature. The case of higher O_2/Coal ratio results in more combustion and leads to lower syngas heating values and higher temperatures. Meanwhile, lower O_2/Coal ratio involves more gasification reactions and results in higher CO concentration and lower temperature. The flow behavior in the gasifier, especially the single fuel injection design on the second stage, is examined and discussed. In summary, the trends of simulated results of coal combustion and gasification processes in the cross-type two-stage gasifier are reasonable and the developed simulation model in this study can be used as a tool for preliminary examination of the global effect of thermal-flow and turbulence on gasification process.

Key words: clean coal technology, gasification modeling, integrated gasification combined cycle (IGCC).

INTRODUCTION

Fuel combustion is usually deemed as the main source of greenhouse gas emission inventories, and it typically contributes over 90% of CO_2 emissions and 75% of total greenhouse gas emissions in developed countries (Garg et al., 2006). In Taiwan, 53.35% of electricity was generated from coal-fired power plants, 20.35% came from LNG-fired (Liquid Natural Gas), 18.10% came from Nuclear power, 3.31% came from oil-fired power plants, while renewable energy, including conventional and pumped storage hydro, generated only 4.9% of electricity in 2009 (BOE, 2010). Coal-fired power plants generate the most electricity, but it also discharges the most CO_2 emissions as contrasting to other electricity utilities. More than 45% of CO_2 emissions were from coal-fired power plants. Therefore, to reduce CO_2 emission, it is important to improve the efficiency of coal-fired power plants or to capture CO_2 from them.

There are many ways to reduce carbon emissions and the associated carbon footprints. Technologies for employing renewable energy such as solar, wind, ocean, hydro, and biomass have been developed and are growing at a fast pace. However, it is undeniable that the most polluted fossil fuel, coal, is still the primary energy source throughout the world. Even in Taiwan, a country without domestic coal production, there is still 34% of energy consumption that comes from coal, in which, 77.62% is utilized for power generation, 1.29% for blast furnace, 8.52% for coke production, and 12.58% for industrial and others (BOE, 2010). The supply of coal is abundant, cheap, stable, and will last for 122 years (BP, 2009). The demand and consumption of natural gas and gasoline have increased during the past few decades. Due to the limited amount of petroleum reserves on the earth, oil prices will expectedly keep growing within the next forty to fifty years. Therefore, the importance of using coal fuel has been emphasized because coal fuels have higher stability and wider variety of sources. However, coal is not considered a clean fuel; thus, future efforts should focus on developing the usages of clean and affordable coal fuel.

Gasification is the process of converting various carbon-based feedstocks to clean synthetic gas (syngas), which is primarily a mixture of hydrogen (H_2) and carbon-monoxide (CO). This conversion is achieved through the reaction of the feedstock with oxygen and steam at a high temperature and pressure with less than 30% of the required oxygen for complete combustion being provided. The syngas produced can be used as a fuel, usually as a fuel for boilers or gas turbines to generate electricity, or it can be used as a source for manufacturing ammonia or hydrogenation applications in refineries to make methanol, hydrogen, or other chemical products. The gasification technology is applicable to any type of carbon-based feedstock, such as coal, natural gas,

* Corresponding Author's E-mail: ypchyou@iner.gov.tw

heavy refinery residues, petroleum coke, biomass, and municipal wastes.

Syngas can be employed in the Integrated Gasification Combined Cycle (IGCC) to produce electricity. Compared to regular or supercritical pulverized coal (SCPC) combustion power plants, IGCC plants can achieve higher efficiency and lower emissions. For power generation, gasification integrated with IGCC is considered a clean and efficient alternative to coal combustion.. The high-pressure and high-temperature syngas from the gasifier can take advantage of the new generation of advanced turbine systems (ATS) to a potential efficiency of more than 50% (LHV). Furthermore, the syngas stream can also be tapped to produce methanol and hydrogen. The gasification technology becomes more important when integrated with carbon capture and sequestration (CCS) technology. CCS is the technology that captures CO_2 by a physical or chemical process and stores it. In a typical case, a fossil-fired power plant implemented with CCS technology can reduce 90% of CO_2 emissions. Because IGCC+CCS capture CO_2 before the syngas combustion, it is easier and cheaper to capture CO_2 compared to PC power plants.

In the next decade, coal-fired power generation will continue to be the main source of electric power in Taiwan; therefore, it is essential to improve the coal combustion efficiency or to develop new technologies such as coal gasification that can extend the usability of coal more cleanly. Before building an experimental gasification facility, this research team is interested in utilizing Computational Fluid Dynamics (CFD) to help understand the thermal-flow and gasification process in the gasifier and guide the design of an experimental gasifier. Hence, the objective of this study is to establish a preliminary coal gasification model to improve the understanding of the gasification processes in a cross-type (E-Gas like) two-stage gasifier as well as to investigate the effects of operating parameters such as slurry concentration and O_2/coal ratio on gasification performance.

LITERATURE REVIEW

In an entrained type gasifier, coal particles are injected into the gasification chamber and mixed with an oxidant stream at a high speed. Under the assumptions of fast chemical reactions and local chemical equilibrium, the reaction and particle movement are dominated by turbulence. Therefore, turbulence models play an important role in coal combustion and gasification simulation, and it affects not only the flow field inside the gasifier but also the coal conversion rate of gasification. Launder & Spalding developed the k-ε model in 1972, and it has since been widely used due to its simple physics and robust feature. Over the past decades a considerable number of models, k-ε model, Reynolds stress model (RSM), large eddy simulation (LES), and direct numerical simulation (DNS), have been developed to study and simulate the turbulent flows.. Hunt & Savill (2004) gave an introduction of the turbulence models and the appropriate conditions to use these models.

The chemical reactions between coal combustion and gasification are similar. Under high temperature, coal is first decomposed through pyrolysis to vaporized volatile substances. With abundant air or oxygen, coal is completely burned to produce carbon dioxide, water, NO_x, SO_x and other trace elements. However, when air or oxygen is insufficient, incomplete or partial combustion occurs, and coal is gasified. In general, coal gasification is categorized for three main steps: (1) devolatilization, (2) volatile combustion and thermal cracking, (3) char combustion and gasification (or char oxidation). The char oxidation is the most important reaction mechanism to produce syngas, which contains complex chemical reactions interacting with the turbulent flow. Because coal combustion has a long history of being applied in industry, the combustion model study is relatively mature. Smoot (1984) and Eaton et al. (1999) comprehensively reviewed the development of coal combustion modeling in fixed, fluidized, and entrained bed. Considering the turbulence, particle dispersion and chemical reaction, Smoot and Smith (1985) and Hill and Smoot (1993) developed a two-dimensional (PGCG-2) and three-dimensional (PGCG-3) pulverized coal combustion model at Brigham Young University. The model solved mass, momentum, and energy conservation equations to simulate coal gasification and combustion. Coal particles under high temperature stream, the heat transfer between dispersed and fluid phases, and the resulting chemical reaction and radiation are illustrated in detail by Smoot & Smith (1985).

The previous studies of coal devolatilization and volatile combustion models developed in the coal combustion models are applied in coal gasification. Comprehensive research has been carried out to understand velocity and temperature distribution as well as syngas composition in the gasification chamber (Chen et al. 2000, Choi et al. 2001, Vicente et al. 2003, and Watanabe & Otaka 2006). Chen et al. (2000a) implemented a three-dimensional model to simulate a 200-ton two-stage air blown entrained type gasifier, developed for an IGCC process. The simulation showed that turbulent fluctuations affected the volatile and char-oxygen reaction and significantly influenced the temperature and gas composition. Chen et al. (2000b) investigated the coal gasification under different parameters such as air ratio and coal particle size. They found that carbon conversion is independent of the devolatilization rate and less sensible to coal particle sizes, but it is sensible to the heterogeneous char-oxygen, char-CO_2 and char-steam reaction kinetics. Besides, air ratio had a significant effect on syngas composition.

The research team at the Energy Conversion & Conservation Center (ECCC) at University of New Orleans has made a significant effort to develop a gasification numerical simulation through the commercial software Ansys/Fluent. Silaen & Wang (2005, 2006, 2009, and 2010) used the geometry and the operating conditions based on the information in Bockelie et al. (2002) and Chen et al. (2000a). They concluded that coal slurry feedstock produced more H_2 than coal powder feedstock, while coal powder feedstock generated more CO. An instantaneous gasification model can provide an overall approach on gasifier performances in terms of temperature, heating value, and gasification efficiency but not adequately catch the local gasification process inside the gasifier. In 2010, they investigated the effects of different turbulence and coal particle size on coal gasification in an entrained-flow gasifier. They concluded that turbulence model significantly influences the gasification results, and only

standard k-ε model and RSM models gave the consistent result in their study. The Kobayashi devolatilization model produces a slower devolatilization rate than the other models. The single rate model and the chemical percolation model produces moderate and consistent devolatilization rate.

MODEL DESCRIPTION

E-Gas (Destec) type Gasifier

The E-Gas™ gasifier consists of two stages, a slagging first stage and an entrained-flow, non-slagging second stage, as shown in Fig. 1. The first stage is a horizontal, refractory-lined vessel in which carbonaceous fuel is partially combusted with oxygen at an elevated temperature and pressure, 2500°F/420 psia (1400°C/29bar). Approximately 80% of preheated slurry and oxygen are fed to each of two opposing mixing nozzles, one on each end of the horizontal section of the gasifier. The geometry is designed to provide a means for thoroughly mixing the reactants and to disperse this mixture, so a high carbon conversion is realized. E-Gas™ has developed its own proprietary design for these slurry mixers. The oxygen feed rate to the mixers is carefully controlled to maintain the gasification temperature above the ash fusion point of 2400 – 2600 °F (1589 – 1700K) (NETL, 2000), ensuring good slag removal and high carbon conversion. The raw fuel gas flows upward into the second (upper) stage of the gasifier while the molten slag flows down the walls of the gasifier and passes into a slag quench bath. In this upper vertical cylindrical stage, the remaining coal slurry is fed to have additional gasification occur and cool down the syngas temperature. The fuel is almost totally gasified in this environment to form syngas consisting principally of hydrogen, carbon monoxide, carbon dioxide and water. Sulfur in the fuel is converted to primarily hydrogen sulfide (H_2S) with a small portion converted to carbonyl sulfide (COS). With appropriate processing downstream, over 98-99% of the total sulfur can be removed from the feedstock prior to combustion in the combustion turbine (NETL, 2000; NETL, 2002).

Descriptions of Baseline Case

Since the exact dimension of the E-Gas gasifier is not known to the authors, a geometry of a cross-type, two-stage gasifier has been built and simulated based on Fig. 1 and the E-gas (Destec) gasification process with feedstock information published in the open literature (NETL, 2000 and 2002). The Fuel properties of the received Illinois #6 Coal are shown in Table 1 and Table 2.

The conditions of coal/water slurry feed, prepared using Illinois #6 coal of the baseline case are shown in Table 3. Approximately 80% of the slurry is gasified / combusted with oxygen in the first (lower) stage using two burners positioned on the opposing ends of this horizontal cylindrical section. In this upper vertical cylindrical stage, only the remaining coal slurry is fed without oxygen. The slurry concentration is 0.67 and O_2/coal ratio is 0.91 for the baseline case. The definition of slurry concentration and O_2/coal ratio in this paper are as follows:

$$\text{Slurry concentration} = \frac{\text{Mass of dry coal (mositure free)}}{\text{Mass of slurry}} \quad (1)$$

$$O_2/\text{Coal} = \frac{\text{Mass of oxygen}}{\text{Mass of coal (MAF, mositure and ash free)}} \quad (2)$$

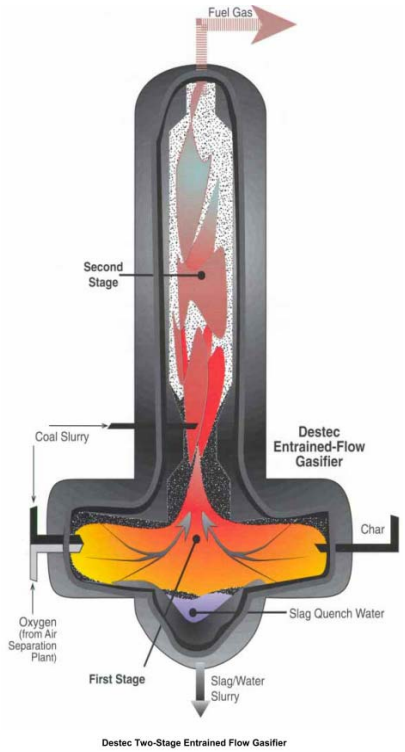

Figure 1 E-Gas (Previous Destec) two-stage entrained flow gasifier. (Source: Destec, 1996)

Table 1 Ultimate analysis of feedstock coal

Ultimate Analysis	Wt. %	Wt. %, dry
Moisture	11.12	
Carbon	63.75	71.72
Hydrogen	4.50	5.06
Nitrogen	1.25	1.41
Chlorine	0.29	0.33
Sulfur	2.51	2.82
Ash	9.70	10.91
Oxygen	6.88	7.75
Total	100	100

Table 2 Proximate analysis of feedstock coal

Proximate Analysis	Wt. %	Wt. %, dry
Moisture	11.12	
Fixed Carbon	44.19	49.72
Ash	9.70	10.91
Volatiles	34.99	39.37
Total	100	100

Table 3 The feedstock conditions of base case

Feedstock conditions of base case	
Flow rate (tons/day)	
- Coal (Wet base):	2550
- Slurry Concentration:	0.67
- ASU O_2/Coal (MAF):	0.91
First Stage Flowrates (tons/day)	4627
- Coal (Dry base, MF):	1793
- H_2O:	896
- O_2	1841
- N_2	97
Second Stage Flowrates (tons/day)	711
- Coal (Dry base, MF):	474
- H_2O:	237
- O_2	0
- N_2	0

METHODOLOGY

Governing Equations

The equations for conservation of mass, conservation of momentum, and energy equations are given as:

$$\nabla \cdot (\rho \vec{v}) = S_m \tag{3}$$

$$\nabla \cdot (\rho \vec{v}\vec{v}) = -\nabla p + \nabla \cdot \left(\overline{\overline{\tau}}\right) + \rho \vec{g} + \vec{F} \tag{4}$$

$$\nabla \cdot \left(\vec{v}(\rho E + p)\right) = \nabla \cdot \left(\lambda_{eff} \nabla T - \sum_j h_j \vec{J}_j + \left(\overline{\overline{\tau}}_{eff} \cdot \vec{v}\right)\right) + S_h \tag{5}$$

where λ_{eff} is the effective conductivity ($\lambda+\lambda_t$, where λ_t is the turbulence conductivity) and J_j is the diffusion of species j.

The stress tensor $\overline{\overline{\tau}}$ is given by

$$\overline{\overline{\tau}} = \mu\left[\left(\nabla \vec{v} + \nabla \vec{v}^T\right) - \frac{2}{3}\nabla \cdot \vec{v} I\right] \tag{6}$$

where μ is the molecular dynamic viscosity, I is the unit tensor, and the second term on the right-hand side is the effect of volume dilatation. The first three terms on the right-hand side of equation (5) represent heat transfer due to conduction, species diffusion, and viscous dissipation. S_h is a source term including the enthalpy formation from the chemical reaction of the species. The energy E is defined as

$$E = h - \frac{p}{\rho} + \frac{v^2}{2} \tag{7}$$

where h is the sensible enthalpy and for incompressible flow and is given as

$$h = \sum_j Y_j h_j + \frac{p}{\rho} \tag{8}$$

Y_j is the mass fraction of species j and

$$h = \int_{T_{ref}}^{T} c_{p,j} dT \tag{9}$$

where T_{ref} is 298.15 K.

Turbulence Models

Standard k-ε Model – The standard k-ε model, based on the Boussinesq hypothesis, relates the Reynolds stresses to the mean velocity as

$$-\rho\overline{u_i' u_j'} = \mu_t\left(\frac{\partial u_i}{\partial x_j} + \frac{\partial u_j}{\partial x_i}\right) - \frac{2}{3}\rho k \delta_{ij} \tag{10}$$

where k is the turbulent kinetic energy, and μ_t is the turbulent viscosity given by

$$\mu_t = \rho C_\mu k^2 / \varepsilon \tag{11}$$

where C_μ is a constant and ε is the dissipation rate. The equations for the turbulent kinetic energy (k) and the dissipation rate (ε) are:

$$\frac{\partial}{\partial x_i}(\rho u_i k) = \frac{\partial}{\partial x_i}\left[\left(\mu + \frac{\mu_t}{\sigma_k}\right)\frac{\partial k}{\partial x_i}\right] + G_k - \rho\varepsilon \tag{12}$$

$$\frac{\partial}{\partial x_i}(\rho u_i \varepsilon) = \frac{\partial}{\partial x_i}\left[\left(\mu + \frac{\mu_t}{\sigma_\varepsilon}\right)\frac{\partial \varepsilon}{\partial x_i}\right] + C_{1\varepsilon} G_k \frac{\varepsilon}{k} - C_{2\varepsilon}\rho\frac{\varepsilon^2}{k} \tag{13}$$

The term G_k is the generation of turbulence kinetic energy due to the mean velocity gradients.

The turbulent heat flux and mass flux can be modeled with the turbulent heat conductivity (λ_t) and the turbulent diffusion coefficient (D_t), respectively.

$$\rho c_p \overline{u_i' T'} = -\lambda_t \frac{\partial T}{\partial x_i} = -c_p \frac{\mu_t}{\mathrm{Pr}_t}\frac{\partial T}{\partial x_i} \tag{14}$$

$$\rho\overline{u_i' C'} = -\rho D_t \frac{\partial C}{\partial x_i} = -\frac{\mu_t}{\mathrm{Sc}_t}\frac{\partial C}{\partial x_i} \tag{15}$$

The constants $C_{1\varepsilon}$, $C_{2\varepsilon}$, C_μ, σ_k, and σ_ε used are: $C_{1\varepsilon}$ = 1.44, $C_{2\varepsilon}$ = 1.92, C_μ = 0.09, σ_k = 1.0, σ_ε=1.3. The turbulence Prandtl number, Pr_t , is set to 0.85, and the turbulence Schmidt number, Sc_t , is set to 0.7.

Reaction Model

Coal gasification reactions occur when coal is heated with limited oxygen and steam in a gasification reaction

chamber. The main global reactions in a gasification process are as follows:

Heterogeneous (solid and gas) phase

$$C(s) + \tfrac{1}{2}O_2 \rightarrow CO, \Delta H^\circ_R = -110.5 \text{ MJ/kmol} \quad \text{(R1)}$$

$$C(s) + CO_2 \rightarrow 2CO, \Delta H^\circ_R = +172.0 \text{ MJ/kmol} \quad \text{(R2)}$$

(Gasification, Boudouard reaction)

$$C(s) + H_2O(g) \rightarrow CO + H_2, \Delta H^\circ_R = +131.4 \text{ MJ/kmol} \quad \text{(R3)}$$

(Gasification)

Homogenous gas phase

$$CO + \tfrac{1}{2}O_2 \rightarrow CO_2, \Delta H^\circ_R = -283.1 \text{ MJ/kmol} \quad \text{(R4)}$$

$$CO + H_2O(g) \rightarrow CO_2 + H_2, \Delta H^\circ_R = -41.0 \text{ MJ/kmol} \quad \text{(R5)}$$

(Watershift)

$$CH_{2.760}O_{0.262} \rightarrow 0.262CO + 1.011H_2 + 0.123C_6H_6 \quad \text{(R6)}$$

(Volatiles cracking)

$$C_6H_6 + 3O_2 \rightarrow 6CO + 3H_2 \quad \text{(R7)}$$

(Volatiles gasification via C_6H_6)

Reactions given in R1 and R4 are two exothermic reactions that provide the complete energy for the gasification. Based on these global reactions, approximately 22% of the stoichiometric oxygen is required to provide sufficient energy for gasification reactions. In real applications, 25~30% of the stoichiometric oxygen is provided to ensure high-efficient carbon conversion.

Partial combustion occurs when the coal mixes with oxygen (R1). The energy released from (R1) also heats up any coal that has not burned. When the coal is heated without oxygen, it undergoes pyrolysis during which phenols and hydrocarbon gases are released. At the same time, char gasification (R2) takes place and releases CO. If a significant amount of steam exists, gasification (R3) and water shift reaction (R5) occur and release H_2. Reactions (R6) and (R7) involve volatiles. The volatiles are modeled to go through a thermal cracking (R6) and gasification processes (R7) via C_6H_6. The enthalpy of volatiles is calculated from the coal heating value and fully combustion of the carbon from the proximate analysis.

The global reaction mechanism is modeled to involve the following chemical species: C, O_2, N_2, CO, CO_2, H_2O, H_2 and volatiles (see reactions R1 through R7). All of the species are assumed to mix in the molecular level. In this study, the instantaneous gasification and equilibrium models will be established. The instantaneous model assumes that coal vaporizes very fast into gas without going through heterogeneous finite-rate reaction process. The equilibrium model will follow the conventional equilibrium concept by incorporating the equilibrium constants into the CFD simulation. The interphase exchange rates of mass, momentum and energy are assumed to be infinitely fast. Carbon particles are made to gasify instantaneously; therefore the solid-gas reaction process can be modeled as homogeneous combustion reactions. This approach is based on the locally-homogeneous flow (LHF) model proposed by Faeth (1987), implying infinitely-fast interphase transport rates. The instantaneous gasification model can effectively reveal the overall combustion process and results without dealing with the details of the otherwise complicated heterogeneous particle surface reactions, heat transfer, species transport, and particle tracking in turbulent reacting flow. The eddy-dissipation model is used to model the chemical reactions. The eddy-dissipation model assumes the chemical reactions are faster than the turbulence eddy transport, so the reaction rate is controlled by the flow motions.

Solution Methodology

The CFD solver used in this study is the commercial CFD code ANSYS FLUENT V.12.0. FLUENT is a finite-volume-based CFD solver written in C language and has the ability to solve fluid flow, heat transfer and chemical reactions in complex geometries, and supports both structured and unstructured meshes. Buoyancy induced flow is calculated. The density in the buoyancy term in the momentum equation is calculated using the ideal gas law.

The segregated solution method is used. Segregated solution solves the governing equations of continuity, momentum, energy, and species transport sequentially (segregated from one another). The non-liner governing equations are linearized implicitly with respect to the dependent variables. The second-order discretization scheme is applied for the momentum, the turbulence kinetic energy, the turbulence kinetic dissipation, the energy, and all the species. The SIMPLE algorithm is used in this study as the algorithm for pressure-velocity coupling. The built-in standard k-ε turbulence model is used.

Boundary Conditions

The schematic diagram of investigated gasifier is shown in Fig. 2. The height of the whole gasifier is 12m, and the length of the horizontal section (1st stage) is 8m. The diameter of the horizontal section is 2m, and the one of the vertical section that includes a convergent-divergent section is 1.6m. There are two opposing inlets in the horizontal section with a height of 1m, while there is only one inlet in the vertical section with a height of 3.6m.

The feedstock of the fuel is about 2550 ton/day with a 0.67 coal slurry concentration and a 0.91 O_2/coal ratio. The inlet temperature of both coal slurry and oxidant is 425K, and the operating pressure is 28atm. The wall is assumed as no slip condition and adiabatic wall condition. The grid-independent studies have been tested in this study. However, even the mesh quantities grow to 2 million, the grid-independent is still not achieved. In order to save the computer resource, there are 1.05 million unstructured meshes used in the computational domain.

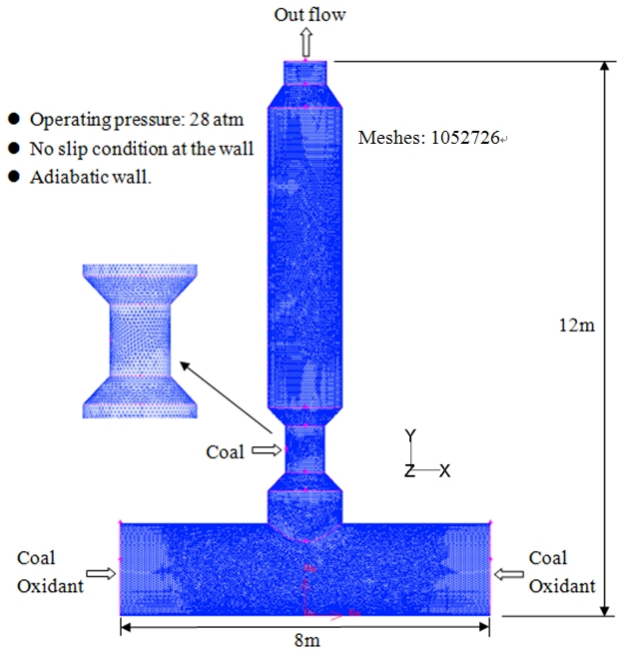

Figure 2 Computational grid and boundary conditions

Grid Sensitivity study

A grid sensitivity study is conducted by using four different grids: 120,000 meshes, 300,000 meshes, 680,000 meshes, and 105,000,000 meshes. Fig. 3 shows the temperature distribution along the gasifier height of the four different grids. In most part the temperature increases as the mesh number increases. The result of 680k grid almost coincides with that of 1.05M grid except in the region near the second fuel injection (height 4~6 m), where the largest temperature difference is about 40K or less than 3%. Considering the difference in most of the area is less than 1%, the 1.05M grid is then used in this study.

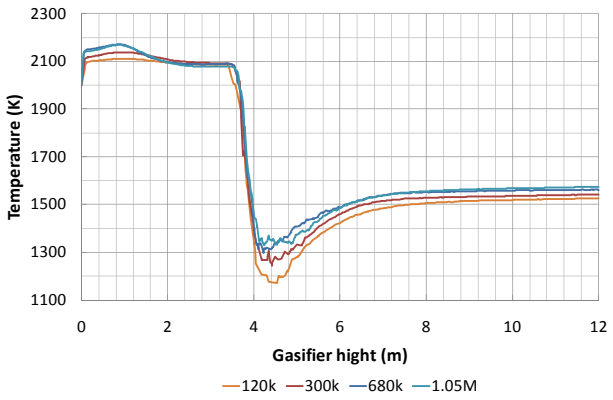

Figure 3 Grid sensitivity of vertical temperature distribution.

RESULTS AND DISCUSS

Baseline Case

Figure 4 shows the velocity contours and vectors along x-y plane at z=0 in the gasifier of the baseline case. The velocity vectors in each circle show the velocity field in a cutting-plane of the gasifier. The results show that the flow is injected strongly in the core of the 1st stage; however, there is backflow in the outer rim region of the bottom vessel. The four cutting-plane vectors of the bottom vessel show the backflow forms an annular recirculation region surrounding the jet core flow in the bottom cylinder on both ends. The slow-moving recirculation zones occupy a portion of the gasifier like blockages and reduce the effective area for the core flow to pass through. This leads to a longer residence time for the flow trapped in the recirculation zones but accelerates the core flow due to reduced effective through-flow area in the 1st stage.

When the raw fuel gas produced in the 1st stage flows upward into the 2nd stage of the gasifier, it is accelerated through the converging throat region. Since there is an inlet feeding with coal slurry in this throat region, the flow field is deflected by the fuel jet and two separated-flow recirculation zones immediately form downstream of the second stage fuel jet locations. Each of these two recirculation zones contains a pair of counter-rotating vortices as shown in the third cross-sectional velocity vector plot from top of Fig. 4. Due to the large include-angle of the divergent section immediately downstream of (or above) the throat, the recirculation zones sustain about three throat-diameters above the second fuel injection location and the flow reattaches to the wall at around 7 meter high of the gasifier. These recirculation zones increase the residence time of the trapped flow and provide well mixing between the unreacted coal slurry and the hot gases from the 1st stage. The lengthened residence time seems beneficial for allowing more thorough reactions, but the yield is low in this region because the produced syngas wastes time recirculating inside this region and does not effectively contribute to the syngas production rate at exit of the gasifier. Therefore, these recirculations actually exert a non-ideal condition because they lengthen only a small part of mass flow in these dead-flow regions and force the main-body flow move faster with less residence time by reducing the effective cross-section area of the flow passage. The accelerated main flow results in requiring a longer gasifier chamber to achieve satisfactory residence time. This uneven distribution of flow fields and residence times leads to the consideration of using multiple tangential jets in the second stage, which can provide a uniformly distributed spiraling flow field with evenly lengthened residence time. In this manner, the length of the gasifier chamber could be shortened and the cost reduced. Another option to reduce the recirculation zones volumes is to reduce the divergent section included angle by increasing the throat area.

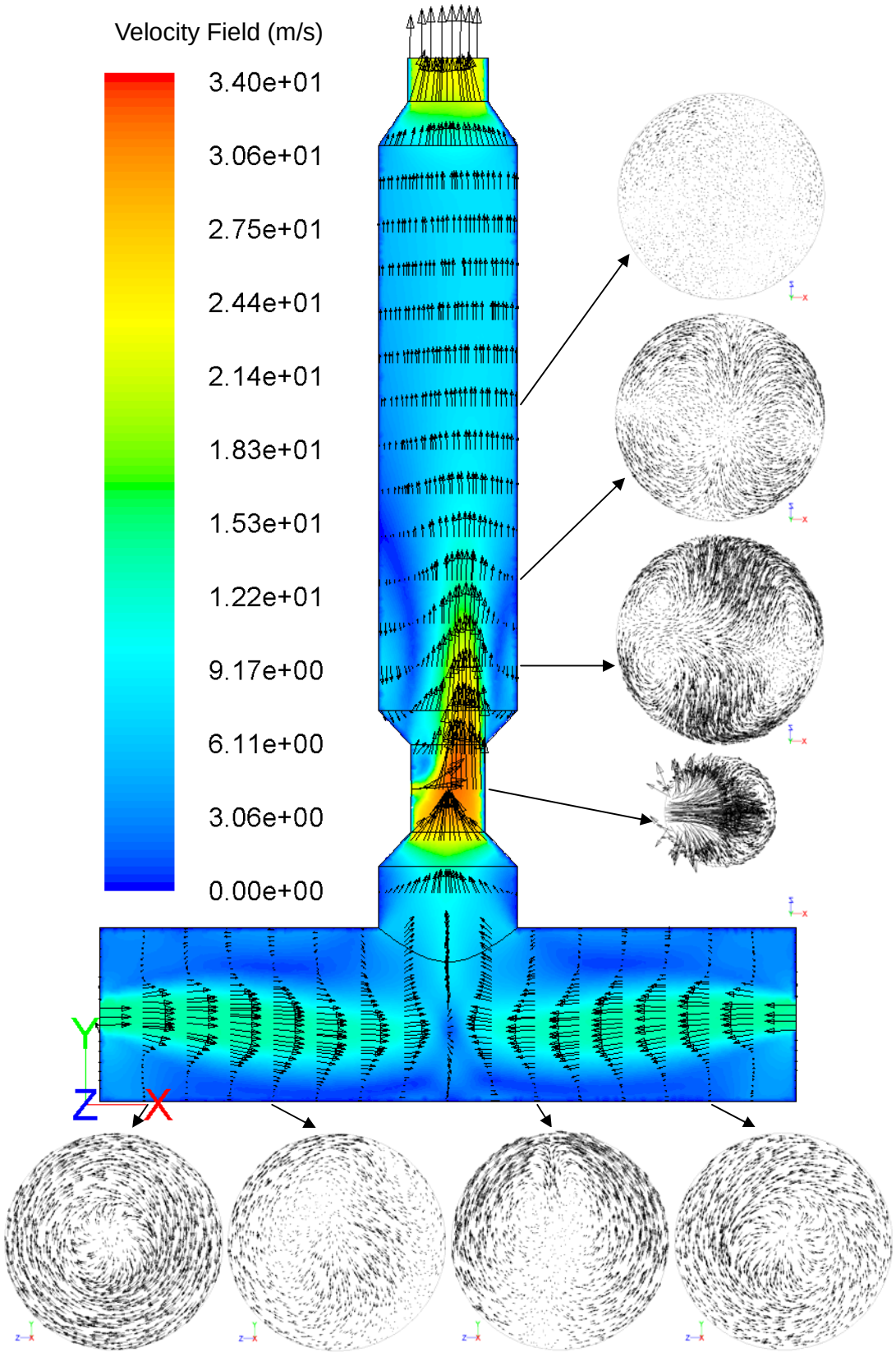

Figure 4 The velocity contours and vectors along x-y plane at z=0 in the gasifier of the baseline case.

Figure 5 shows the flow pathline in the gasifier. As the pathline diagram indicates, the gas injected into the gasifier from the opposing inlets in the horizontal section causes a strong upward flow in the middle of the 1st stage. Then most of the fluid turns an angle of 90 degrees and flows upward to the gasifier outlet. The residence time of the fluid from inlet to outlet ranges from 1.15 to 26.6 seconds. However, it can be seen that in the computational domain, the majority of the pathline colors are blue and turquoise ranging between 2 and 6 seconds, and few pathline showing longer residence time in green, yellow, and red. These are the fluid particles that have hung around recirculated for a couple of times before flowing to the outlet. Generally speaking, the residence time of an entrain-bed type gasifier is usually in the scale of seconds, and the result of the 2 – 6 seconds residence time seems to be reasonable.

Figure 6 shows the 3-D temperature contours of the gasifier. Figure 7 shows the contours of temperature and mole fractions of CO_2, CO and H_2 along x-y plane in the gasifier. Combustion occurs when coal slurry and oxidant are injected into the first stage. The carbon and the oxygen react immediately and generate CO via R1 reaction. Then CO reacts with oxygen again to produce CO_2 via R4 reaction. The oxidation and combustion reactions generate significant heat and the temperature in the middle of first stage is raised to over 2300K. Due to the feed of oxygen being insufficient for full combustion, some of the coal is consumed and converts into CO and H_2 via gasification process by reacting with CO_2 and H_2O via R2 and R3 reactions. Because these two equations are endothermic reactions, the temperature in the exit of bottom vessel is lowered to around 2000K.

When the hot raw syngas transports into the upper stage, it reacts with the coal slurry, which is fed from the upper jet. There is no additional oxidant being fed into the second stage, so the main reaction in this region is gasification. More CO and H_2 are produced in this section. When syngas exits the gasifier, the temperature is cooled down to 1591K, due to endothermic gasification process and the mole fractions of H_2 and CO are raised to 0.417 and 0.372, respectively.

The exit temperature of E-gas gasifier is 1311K according to open literature [NETL, 2000]; however, the predicted value in the base case is 1591K. The difference between the simulation and the actual operation of E-gas gasifier is due mainly to the following causes: (1) The wall of gasifier is set to be adiabatic, which implies that there is no heat loss through the wall boundary; (2) The devolatilization process has not been implemented in this study; thus the energy needed to drive out the volatiles are not consumed.

Due to the fast reaction in the eddy-dissipation model, there is no H_2O remained in the exit syngas. The mole fraction of H_2 in the simulation results is also higher than the counterpart documented in the NETL report (2000).

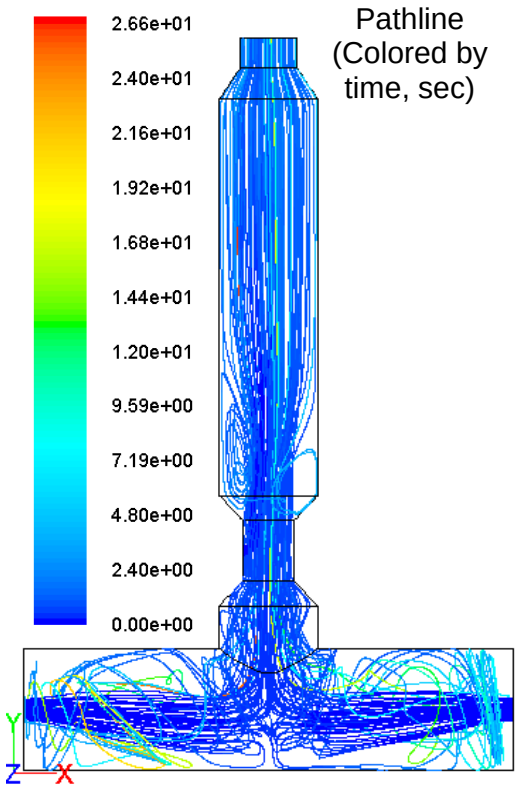

Figure 5 Flow pathlines of the gasifier.

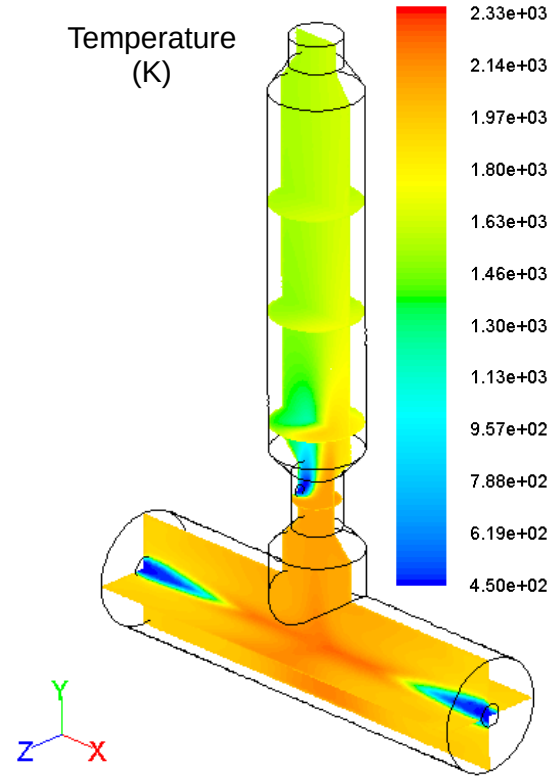

Figure 6 3-D temperature contours of the gasifier.

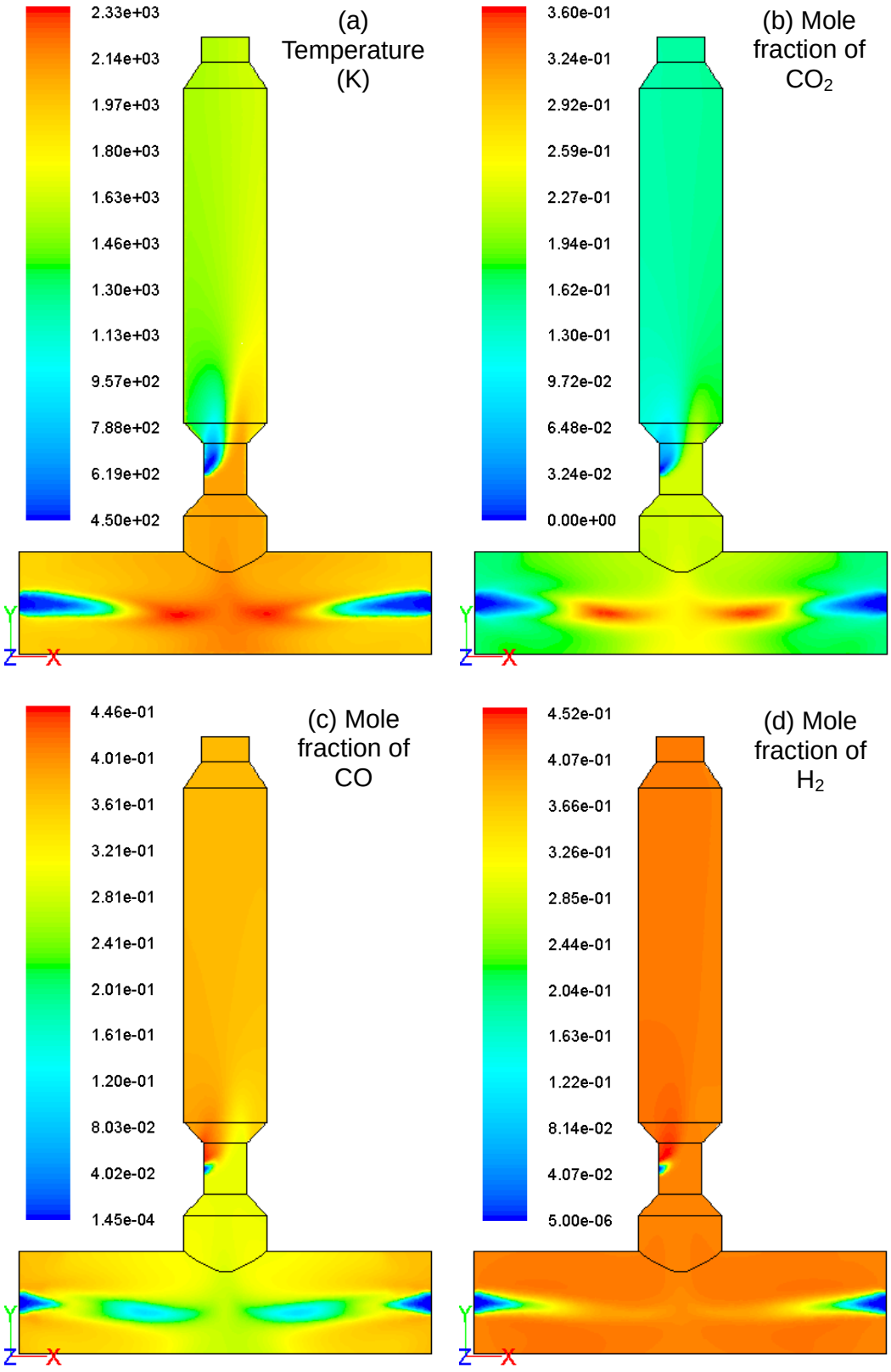

Figure 7 The contours of temperature and mole fractions along x-y plane in the gasifier of baseline case.

Effects of Slurry Concentration

Cases A1 to A5 in Table 4 are the cases showing the effects of slurry concentration of gasification process. In the coal slurry concentration series cases, the weight of feeding coal and oxidant are fixed; higher value of coal slurry concentration indicate less water in the slurry.

Table 4 The input conditions and simulation results showing effects of slurry concentration on gasification.

		Case A1	Case A2	CaseA3 Baseline Case	Case A4	Case A5
O_2/Coal		0.91	0.91	0.91	0.91	0.91
Coal/Slurry		0.55	0.6	0.67	0.75	0.8
Temperature (K)		1424	1494	1591	1675	1722
Mole Fraction (%)	CO	25.0	30.7	37.2	45.4	50.1
	H_2	47.7	45.0	41.7	37.8	35.5
	CO_2	22.1	18.7	14.9	10.1	7.4

The results in Table 4 show that when the value of coal slurry increases (i.e., less water), the mole fraction of CO increases, and on the contrary, the mole fraction of H_2 becomes lower due to less water in the feedstock. However, when the value of coal slurry decreases (i.e., more water), the mole fraction of CO_2 becomes higher, but the temperature decreases. When there is more water in the feedstock, more carbon reacts with H_2O as well, which generates CO and H_2 via R3 reaction. Then CO reacts with H_2O and generates CO_2 and H_2 via R5 reaction. In the results, there are more R2, R3 and R5 reactions in lower slurry concentration cases comparing to higher concentration cases, especially more R3 and R5 reactions. Although carbon will react with CO_2 to generate CO via R2 reaction, the concentration of carbon is less in low slurry case, there is also less carbon to react with CO_2 via R2 reaction comparing with R3 and R5 reactions. This leads to more CO_2, more H_2 and less CO produced in the low slurry case.

The results show that the temperature decreases with reduced slurry concentration. The temperature of exit syngas in Case A1 is 1424K and in Case A5 is 1722K. The equation R5 is an exothermic reaction, but there are more endothermic reactions, R2 and R3, which deplete more energy. This is the reason why the exit temperature of Case A1 is lower than that in other high slurry concentration cases. In summary, Table 4 shows lower slurry (or more water) produces more CO_2 and provides the syngas with higher concentration of H_2 and lower concentration of CO.

Effects of Oxygen / Coal ratio

Cases B1 to B5 in Table 5 show the results of the effects of O_2/coal ratio. In the O_2/coal series cases, the weight of feeding coal and water are fixed; higher value of O_2/coal ratio indicates more oxidant in the feedstock.

Table 5 The input conditions and simulation results showing effects of O_2/coal ratio on gasification process.

		Case B1	Case B2	CaseA3 Baseline Case	Case B4	Case B5
O_2/Coal		0.85	0.88	0.91	0.95	0.98
Coal/Slurry		0.67	0.67	0.67	0.67	0.67
Temperature (K)		1448	1521	1591	1684	1750
Mole Fraction (%)	CO	38.6	37.9	37.2	36.3	35.6
	H_2	42.1	41.9	41.7	41.5	41.3
	CO_2	13.2	14.1	14.9	16.0	16.9

Equations R1, R4 and R7 are the main exothermic reactions in the gasification process. When O_2/coal ratio increases, there is more oxygen for R1, R4 and R7 reactions, and the temperature of the exit syngas becomes higher. The purpose of the gasification process is to reduce the combustion process and generate more syngas, i.e., CO and H_2. When the input oxygen concentration is higher, there is more combustion reaction with less syngas production. However, the energy for devolatilizing and thermally cracking coal is from the combustion process. If there isn't enough oxygen for the combustion process, there will be insufficient energy for gasification process, and the syngas production will be less. More oxygen is helpful for the combustion process and leads to higher temperatures in the gasifier. The exit temperature increases with elevated O_2/coal ratio. In Case B1, due to the lack of oxygen input into the gasifier, the temperature is lower than in other cases. The temperature of exit syngas is 1448K in case B1 and 1750K in Case B5.

The mole fractions of CO, H_2 and CO_2 are shown in Table 5. When there is more oxygen in the gasifier, there is also more CO_2 generated from the combustion process via R4 reaction; meanwhile, the mole fraction of CO is less. The change of H_2 from Case B1 to B5 is not distinct. The source of H_2 is mainly from Char-H_2O gasification. In the O_2/Coal series cases, the feedstock of coal and water are fixed. The only changes in the series cases are oxygen inputs. So the change of H_2 is not obvious in the O_2/coal series cases.

Comparison with the EPA data

Table 6 shows that the operating parameters used in this paper include the operating conditions published in NETL (2000) and EPA (Nexant, 2006). The slurry concentration varies from 0.55 to 0.80, and the O_2/Coal ratio varies from 0.85 to 0.98. It can be seen that the simulating parameters used in this paper are consistent with an actual working gasifiers.

Table 6 Operating parameters in the simulated cases

Coal(MF)/Slurry \ O_2/Coal(MAF)	0.85	0.88	0.91	0.95	0.98
0.55			x		
0.60			x		
0.64			x		x(EPA)
0.67	x	x	x(NETL)	x	x
0.75			x		
0.80			x		

Table 7 shows the comparison of outlet species mole fraction with EPA results, which are computed by Aspen Plus. The major difference is the H_2O mole fraction. The outlet species concentrations of H_2 and CO_2 in this study are higher than EPA results, while the values of CO and H_2O in this study are lower than EPA results. And according to the R5 reaction, CO reacts with H_2O and produces CO_2 and H_2. It can be judged that the major difference is caused by the water shift reaction rate of R5. It is clear that the water-shift reaction rate is too fast in the current model using the eddy-dissipation model. Implementation of a correct finite-rate model for water-shift reaction is essential for achieving a more accurate prediction. This will be left as a future task for this research.

Table 7 The comparisons of simulated results with EPA's results.

Mole fraction (%)	Simulated results	EPA's results
CO	32.2	42.3
H_2	42.8	30.7
CO_2	19.1	9.6
H_2O	0.0	14.9

CONCLUSION

A three-dimensional computational model has been established to simulate the coal combustion and gasification in a cross-type two-stage gasifier. The instantaneous gasification model is adapted in this study to investigate the gasification processes. The instantaneous gasification model significantly reduces the computational time but can only provide a qualitative trend of gasification process for preliminary investigation. Although the instantaneous gasification model is simplified, it can adequately capture the global feature of the effect of the thermal-fluid field (including turbulence structure) on chemical reactions.

The results show that when the value of slurry concentration (carbon to water ratio) increases, the temperature of exit syngas is also higher. When the slurry concentration is lower, there are more R2, R3 and R5 reactions and leads to a higher concentration of H_2 and CO_2; meanwhile, the concentration of CO and temperature is lower. Under the condition of feeding carbon being nearly completely converted, low slurry concentration is preferred over high concentration if more H_2 is wanted with lower syngas temperature, while higher slurry concentration is more preferable for producing more CO with higher syngas temperature and less CO_2. Higher O_2/coal ratio also leads to higher temperature. When the higher O_2/coal ratio, there is more combustion reaction and generates more CO_2. The effect of O_2/coal ratio on H_2 production is not obvious, especially for a high O_2/coal ratio.

The single jet injection in the second stage induces large recirculation regions, which introduces inefficiency and reduced syngas production by trapping a portion of the flow, reducing the effective flow passage area, speeding up the main flow, and decreasing the residence time of main flow. An alternate design of using multiple tangential jets injections in the second stage or enlarging the throat diameter can be considered.

Although the simplified instantaneous gasification model is used in this study, the trends of simulated results of the coal combustion and gasification process in the cross-type, two-stage gasifier are reasonable. Future activities need to be considered in the finite-rate reaction mode, especially the water-shift reaction rate without catalysts, and investigate the effects of turbulent model on the gasification process.

ACKNOWLEDGEMENTS

The authors are grateful to National Science Council of TAIWAN ROC for the financial support of the code number NSC 98-3114-Y-042A-005.

REFERENCES

BOE (Bureau of Energy), (2010). Energy Statistical Hand Book 2009. Bureau of Energy, R.O.C. (in Chinese).

Bockelie, M.J., Denison, K.K., Chen, Z., Linjewile, T., Senior, C.L., Sarofim, A.F., (2002). CFD modeling for entrained flow gasifiers in vision 21 systems, Ninteenth International Pittsburgh Conference, Pittsgurgh, PA, USA.

BP, (2009). BP Statistical Review of World Energy. BP.

Chen, C., Horio, M. & Kojima, T., (2000a). Numerical simulation of entrained flow coal gasifiers. Part I: modeling of coal gasification in an entrained flow gasifier. Chem. Eng. Sci., 55, 3861-3874.

Chen, C., Horio, M. & Kojima, T., (2000b). Numerical simulation of entrained flow coal gasifiers. Part II: effects of operating conditions on gasifier performance. Chem. Eng. Sci., 55, 3875-3883.

Choi, Y. C., Li, X. Y., Park, T. J., Kim J. H. & Lee, J. H., (2001). Numerical study on the coal gasification characteristics in an entrained flow coal gasifier. Fuel, 80, 2193-2201.

Destec Energy, Inc., (1996). The Wabash River Coal Gasification Repowering Project. TOPICAL REPORT NUMBER 7, NOVEMBER 1996.

Eaton, A. M., Smoot, L. D., Hill S. C. & Eatough C. N., (1999). Components, formulations, solutions, evaluation and application of comprehensive combustion models. Prog. Energy Combust. Sci., 25, 387-436.

Faeth, G.M., (1987). Mixing, Transport and Combustion in Sprays, Progress in Energy Combustion Science, Vol. 13, pp. 293-345.

Garg, A., Kazunari, K., and Pulles, T., (2006). 2006 IPCC Guidelines for National Greenhouse gas Inventories, Chapter 1: Introduction. The Intergovernmental Panel on Climate Change (IPCC).

Hill, S.C. and Smoot, L.D., (1993). A Comprehensive Three-Dimensional Model for Simulation of Combustion Systems: PCGC-3, Energy & Fuels, 7, 874-883.

Hunt, J. C. R. & Savill, A. M., (2004). Guidelines and criteria for the use of turbulence models in complex flows. In Prediction of Turbulence Flows, eds. G. F. Hewitt and J. C. Vassilicos, Cambridge University Press, Cambridge

Jones, W.P., and Lindstedt, R.P., (1988). Global Reaction Schemes for Hydrocarbon Combustion, Combustion and Flame, 73, 233-249.

Launder, B. E. & Spalding, D. B., (1972). Lectures in mathematical models of turbulence. New York, Academic Press

NETL, (2000). Destec Gasifier IGCC Base Cases, PED-IGCC-98-003.

NETL, (2002). The Wabash River Coal Gasification Repowering Project: A DOE Assessment, DOE/NETL-2002/1164.

Nexant, Inc., (2006). Environmental Footprints and Costs of Coal-Based Integrated Gasification Combined Cycle and Pulverized Coal Technologies, United States Environmental Protection Agency (EPA), EPA Contract No. 68-W-03-33, Work Assignment 2-02.

Silaen, A. & Wang, T., (2005). Simulation of coal gasification inside a two-stage gasifier. Twenty-Second International Pittsburgh Conference, Pittsgurgh, PA, USA.

Silaen, A. & Wang, T., (2006). Effects of Fuel Injection Angles on Performance of A Two-Stage Coal Gasifier. Twenty-Third International Pittsburgh Conference, Pittsgurgh, PA, USA.

Silaen, A. & Wang, T., (2009). Comparison of Instantaneous, Equilibrium, and Finite-rate Gasification Models in an Entrained-flow Coal Gasifier. Twenty-Sixth International Pittsburgh Conference, Pittsgurgh, PA, USA.

Silaen, A. & Wang, T., (2010). Effect of turbulence and devolatilization models on coal gasification simulation in an entrained-flow gasifier. International Journal of Heat and Mass Transfer 53, 2074–2091.

Smoot, L. D., (1984). Modeling of coal-combustion processes. Prog. Energy Combust. Sci., 10, 229-272

Smoot, L. D. & Smith, P. J., (1985). Coal combustion and gasification. Plenum Press, New York

Vicente, W., Ochoa, S., Aguillon, J. & Barrios, E., (2003). An Eulerian model for the simulation of an entrained flow coal gasifier. Appl. Therm. Eng. 23, 1993-2008

Watanabe, H. & Otaka, M., (2006). Numerical simulation of coal gasification in entrained flow coal gasifier. Fuel, 85, 1935-1943